Optimising composition and spatial deployment of diversity in agricultural crops for disease control and yield enhancement

Problem brought by Adrian Newton
Adrian.Newton@scri.ac.uk
Scottish Crop Research Institute,
Invergowrie, Dundee, DD2 5DA, Scotland, UK.

Report by Zofia Jones[†], Jonathan Wattis[†], Jonathan Hiorns[†] & Ibrahim Taha[‡]
pmxzj1@nottingham.ac.uk Jonathan.Wattis@nottingham.ac.uk
pmxjh1@nottingham.ac.uk elmojtaba@gmail.com
[†]Centre for Mathematical Medicine, School of Mathematical Sciences,
University of Nottingham, University Park, Nottingham NG7 2RD, UK.
[‡]Faculty of Mathematical Sciences, University of Khartoum, Sudan.

Other contributors during the study group:
Marianna Cerasuolo[§] & Katarzyna Oles[¶]
Marianna.Cerasuolo@bbsrc.ac.uk kas@cs.stir.ac.uk
[§]Rothamsted Research, West Common,
Harpenden, Hertfordshire, AL5 2JQ, UK.
[¶]Department of Computer Science & Mathematics,
University of Stirling, Stirling, FK9 4LA, Scotland, UK.

Latest version: April 12, 2010

Contents

1 Introduction

There is only demand in the market for a limited variety of a particular crop such as barley or wheat. However, genetic and phenotypic diversity has been found to increase yield and resistance to pestilence. To ensure a good yield when planting monocultures farmers rely on pesticides and fertilisers which can be costly and harmful to wildlife.

Agricultural scientists at the Scottish Crop Research Institute (SCRI) have conducted experiments to find quantitative data on the yield and resistance to fungal infection of barley for different types of crop pattern. Yield can be quantified by the weight of the harvest per area of field or amount of seed. Two fungal infections which commonly infect barley are mildew and rynchosporium, known as "ryncho". The degree of infection by these fungi is quantified on a scale of 1-9 which is assigned to each plot after careful observation. The scale roughly relates to a percentage of the crop which is infected as given in Table.1. Varieties of barley are planted as either monocultures with one type of barley in a field, as homogenous mixtures where different types of seed are put into a mixer before planting or in a checkered pattern when the field is divided into a grid of equally sized plots. We refer to this last technique as patched planting. Their data indicate that planting different varieties of crop in the same field increases both yield and resistance to disease. Patch size is expected to influence these effects, since the limit of small patch size corresponds to a homogeneous mixture, whilst large a patch size approximates a monoculture. It is expected that the positive effects will be maximised at some plot size.

There are two separate measurable effects of varying the planting patterns of barley from that of a monoculture: the increase in yield and the decrease in pestilence. These effects can be modelled separately. The increase in yield can partly be accounted for by the decrease in pestilence. However, letting different varieties of barley grow in the same field can also increase the yield by allowing the different varieties to exploit different environmental niches. Different varieties may have different root lengths or different nutritional preferences so that all the plants are not competing for the same water and mineral resources. However, it is known that plants quickly adapt, so a given set of environmental conditions will determine the observable characteristics of a plant more than their genotypes. It has been observed that when different varieties of barley are planted in the same field the heights of taller or shorter varieties average out compared to what would be expected in a monoculture. A characteristic which is fixed by the genotype of a variety of barley is its resistance to fungal infection, which is what this report will consider.

Scale	1	2	3	4	5	6	7	8	9
%	0	0.5	1	5	10	25	50	75	100

Table 1: Scale of fungus infection as it related to the percentage of the crop infected.

Mildew is dispersed as a powder by the wind. Different strains of mildew can be divided into clear subgroups. A given variety of barley will have a particular immunity to each given strain of mildew. The exact genes in varieties of barley responsible for this immunity are known. The picture is not so clear for rynchosporium. Unfortunately, the most complete available data is for rynchosporium infection which makes it the preferable case to model.

Ryhchosporium and mildew differ in their mechanisms of dispersion. Rather than being dispersed by the wind, rynchosporium is dispersed by rain splashing off infected leaves and soil contaminated with rynchosporium and onto uninfected plants. Once a rynchosporium spore settles on a leaf it quickly buries itself under the leaf's waxy surface or cuticle. A lesion in the leaf starts to grow as the colony of spores uses the leaf's nutrients to grow. The lesion grows outwards from a

necrotic core. After 10–14 days the colony in a lesion copiously starts producing spores which can infect other plants.

A ryncho colony in any given lesion is a mixture of different strains. The strains do not interact directly but as ryncho spores control the maximum size of their population by chemical signals they effectively compete for resources. Strains can be grouped according to their viability on different crop varieties. There is some indication that ryncho spores can be grouped into three different strains. After two dispersal cycles onto one plant variety, one group would be expected to form 40% of the population [4].

The available data is for five different planting patterns. The first is a monoculture of maris otter barley. The second is a monoculture of manitou barley. The third is a homogenous mixture of both. The fourth and fifth are 1 foot by 1 foot and 4 feet by four feet grids of alternating varieties. Time frequency and intensity of rain drops are also available.

The data gathered must be understood in the context of the life cycle of a crop of barley. Barley planted in September is known as winter barley while barley planted in March is known as spring barley; their life cycles are summarised in Table 2. Over winter, during the November-March period, the rain disperses the fungal spores fairly evenly over the whole crop while keeping down the level of observable disease. It can be clearly observed that the pattern of infection closely reflects the planting pattern. Lesions are mostly found on the plots where the barley is less resistant. The period critical to whether a given crop is mostly inflected or not is the period of rapid growth in May and June, when the stems of the barley shoot up. It is during this period that the pattern of infection breaks out of its winter holding pattern over the whole of the field.

	Winter	Spring
Sep-Nov	Growth	/
Nov-March	Cold/Rain	/
March	/	Planting
March-May	Growth	Growth
May-June	Rapid growth	-stem extension
July	Harvest	/
August	/	Harvest

Table 2: Life cycle of barley

The way in which rain disperses spores across a field may seem complicated. Rain falling down off plants washes spores into the soil, while raindrops rebound off the ground, splashing spores on to surrounding plants. A single plant may have leaves with lesions and also healthy leaves without so that one plant cannot be strictly considered to be one unit. Rain can be considered to be a series of "splash events" with some kind of frequency in space and time. The height and width of dispersal of an individual splash events depends on the volume and velocity of the raindrop and the moisture level in the soil. Some of the rebounding raindrop may be considered aerosolised, allowing it to be dispersed over a larger area. Most of the raindrop will splash upwards, forming a conical shape.

The way in which the lesions are caused by the fungi is also not necessarily simple. Essentially, the colonies use up plant resources which would otherwise be used for the plant to grow and produce grain. The extent to which a plant is affected depends not only on whether the plant is infected or not, but also on the number of lesions. Also, being infected during a time critical for growth will affect the crop more than other times.

From the discussion so far it is clear that there are two separate aspects to model. The first

is the mechanism of physical dispersion of the spores while the second is the extent to which a colony of fungi thrive on a particular variety of barley. If the time taken for a population of rycho to move across a plot of a given width is larger than the time taken for the rycho colonies to be mostly adapted to one variety of barley then the transition from one plot type to the next should slow down the speed of dispersal.

In Section 2 we describe the modelling approach taken and discuss some general models of the crop-pathogen interaction. A more detailed and specific model of pathogen spread is given in Section 2.3; the steady-states for this system are derived in Section 2.5. However, since it is not clear that steady-states will be approached in the timescale of the crop's growth, in Section 2.7 we analyse the dynamics by which pathogens spread. Numerical simulations of the system are illustrated in Section 2.9. Finally we draw conclusions in Section 3.

2 Mathematical modelling

The following physical behaviour should be described in a model:

- **physical dispersal**. We need to consider how to model the spread of the spores by splashing.
- **time lag**. There is a one and a half week period, between when a plant is infected and when more spores are produced and can infect the surrounding plants.
- **competitive advantage**. It is required that species exhibit a variety of different susceptibilities to the different species of Rycho.
- **adaptability**. It is required that the population of spores will change depending on the crop, so the number of spores with the competitive advantage increases.
- **self limiting size of colony**. It is required that the total number of spores doesn't exceed a certain number.

2.1 Combined modelling of crop and pathogen

In mathematical epidemiology, deterministic models are set up by dividing the population into subgroups, the most common being S-I-R models which model subjects who are susceptible, infected and who have recovered from a particular disease. This has numerous generalisations; in one of the more relevant for this case, the appropriate subgroups would be:

- **Susceptible**. Not inflected.
- **Exposed**. Displays symptoms but is not infectious. This is the incubation period that lasts about one and a half weeks.
- **Infectious**. Spores are being produced which can infect other plants.
- **Diseased**. Plants which have lesions. If the plants are infected too badly they shall die.

The disadvantage of such a model is that it does not account for spatially separated models which may interact. Also, this model does not account for the population of the fungus.

Assuming a host (plant) population, of type 1 occupies patch 1, we denote the health of a typical plant by H_1, which we think of as total leaf area, and the population size of a pathogen (fungus)

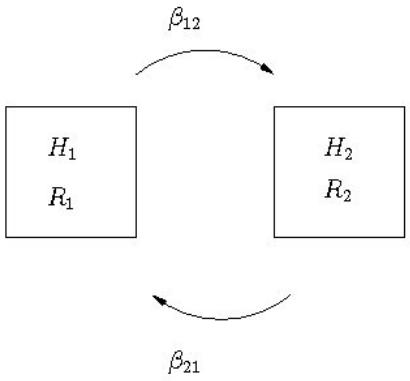

Figure 1: Diagram of interaction between H_1 and R_1 on patch 1 and H_2 and R_2 on patch 2.

population by R_1, while species 2 with health H_2 and pathogen of population size R_2 occupy patch 2 then a simple host-pathogen model with logistic growth can be written as

$$\underbrace{\frac{dH_1}{dt}}_{\substack{\text{rate of}\\ \text{change of}\\ \text{health}}} = \underbrace{a_1 H_1(1-b_1 H_1)}_{\substack{\text{logistic growth}\\ \text{of crop}}} - \underbrace{\alpha_1(H_1,R_1)}_{\substack{\text{deleterious}\\ \text{effect of}\\ \text{pathogen}}}, \tag{1}$$

$$\underbrace{\frac{dR_1}{dt}}_{\substack{\text{rate of}\\ \text{change of}\\ \text{pathogen}}} = \underbrace{c_1 R_1\left(1-\frac{R_1}{K_1(H_1)}\right)}_{\substack{\text{logistic growth}\\ \text{of pathogen on}\\ \text{crop}}} - \underbrace{\beta_{12}R_1(t-\tau)}_{\substack{\text{dispersal to}\\ \text{neighbouring}\\ \text{sites}}} + \underbrace{\beta_{21}R_2(t-\tau)}_{\substack{\text{spread in from}\\ \text{neighbouring}\\ \text{sites}}}, \tag{2}$$

with equivalent equations for patch 2.

Biologically these equations represent the rates of change of the number of host plants or the pathogen. The first term on the right hand side of each equation represents logistic growth. This gives an initial increase in numbers but as the population grows the rate descreases until it reaches the maximum sustainable population size. For the host plants this would be $H_1 = 1/b_1$, while for the pathogen it would be $R_1 = K_1(H_1)$. This therefore takes into account the self limiting size of the colony, as well as its dependence on the area of leaves in the crop, H_1; typically we might expect a simple relationship of the form $K_1(H) = K_0 + K_1 H$. The second term on the right hand side of (1) describes how the interaction of the plants and the pathogen affects the growth of the crop. The host number is reduced at a rate α_1. The final terms in (2) represents the rate at which the pathogen moves from one patch to the other. β_{12} represents the rate at which the the pathogen moves from the first to the second patch, while β_{21} represents the opposite. A time delay of τ is included to represent the time lag between when a plant is infected and when new spores can be produced.

All parameters depend on environmental factors such as temperature (humidity, etc), and as a simple approximation, we will take them to be constant; a slightly more accurate model would allocate one value for each through the winter and an alternative value in the summer.

2.2 The mathematical modelling of pathogen spread

We now concentrate on the spread of the pathogen separate from any effect they may have on the host plants. The transport terms, namely $\beta_{12}R_1(t-\tau)$ and $\beta_{21}R_1(t-\tau)$ can be incorporated into a diffusion term, $\overline{D}$. To simplify later analysis, we take $\tau = 0$.

Let $R(x,t)$ be the number of spores in the small region of width δ centred on x, that is $(x - \frac{1}{2}\delta, x + \frac{1}{2}\delta)$, at time t. We assume that spores can travel a distance δ in time ϵ with probablity p and they have an equal probability of moving to a location with larger or smaller x. Then we have

$$R(x,t+\epsilon) = (1-p)R(x,t) + \tfrac{1}{2}p\left[R(x+\delta,t) + R(x-\delta,t)\right]. \tag{3}$$

assuming that δ and ϵ are both small, taking Taylor series of all terms leads to the partial differential equation

$$\frac{\partial R}{\partial t} = D\frac{\partial^2 R}{\partial x^2}, \tag{4}$$

where $D = p\delta^2/4\epsilon$ is the diffusivity of the spores, that is a measure of how likely they are to move, and how far they move and over what timescale.

Further justifications for using a diffusion term can be found in [3], which also quotes data which can be fitted a mathematical model. Pielaat [3] derive a diffusion term of the form

$$\overline{D} = \frac{\overline{\epsilon}\overline{\lambda}\overline{\sigma}^2}{2}. \tag{5}$$

where

- $\overline{\lambda}$ is the death rate (per time unit) of a spore being splashed during a rain event,
- $\overline{\epsilon}$ is the probability of a spore staying in the the system per splash. Some of the spores could either be washed into the soil or splashed out of the domain,
- $\overline{\sigma}^2$ is the variance of the distribution of distances travelled by spores.

2.3 Proposed model of pathogen spread

As suggested by preliminary experiments, we shall assume that there are three different groups of species of Rhyncho denoted with subscripts 1, 2 and 3. We shall denote the density of each species by $\overline{n}_1$, $\overline{n}_2$ and $\overline{n}_3$, respectively. We shall model the spread of each of the populations over a domain that contains two different varieties of plant, denoted as A and B, which have different levels of susceptibility to each of the different populations. These are assigned in the matrix, $\overline{\alpha}$, which has the form

$$\overline{\alpha} = \begin{pmatrix} \overline{\alpha}_1^A & \overline{\alpha}_1^B \\ \overline{\alpha}_2^A & \overline{\alpha}_2^B \\ \overline{\alpha}_3^A & \overline{\alpha}_3^B \end{pmatrix}, \tag{6}$$

where $\overline{\alpha}_j^X$ denotes the growth rate of species j of pathogen on crops of species X ($j = 1,2,3$, $X = A, B$). In general we shall assume that these parameters are all different, but special cases arise if some are identical.

We shall assume that the pathogen does not spread over the boundaries of the field and we shall assume that the pathogen is inserted at one edge and see how it spreads across the domain. At the boundary of two patches where two species of crop meet, we impose the condition that $\overline{n}_j$ are continuous, and that the spores spread with their usual diffusion rate $\overline{D}$. We assume that the

death rate of pathogen $\overline{\lambda}$ is independent of species and crop, thus $\overline{\lambda}$ will be taken to be independent of space; we make similar assumption on $\overline{D}$.

In one dimension $\overline{n}_1$ satisfies

$$\underbrace{\frac{\partial}{\partial \overline{t}}\overline{n}_1(x,t)}_{\substack{\text{rate of}\\ \text{change of}\\ \text{pathogen pop.}}} = \underbrace{\overline{D}\frac{\partial^2}{\partial \overline{x}^2}\overline{n}_1}_{\substack{\text{diffusive}\\ \text{spread of}\\ \text{pathogen}}} - \underbrace{\overline{\lambda}\overline{n}_1}_{\substack{\text{death of}\\ \text{pathogen}}} + \underbrace{\overline{\alpha}_1^X\,\overline{n}_1\left(1-\frac{\overline{n}_1+\overline{n}_2+\overline{n}_3}{\overline{n}_{\max}}\right)}_{\substack{\text{logistic growth}\\ \text{to maximum total}\\ \text{colony size}}}, \tag{7}$$

where $X = A, B$ depending upon which species of plant the pathogen is growing, with similar equations holding for $\overline{n}_2$ and $\overline{n}_3$. Note that in the logistic growth term, the maximum size of the total colony of all species collectively is $n_1 + n_2 + n_3$.

For a more realistic model of spread in a two-dimensional field the operator $\partial_{\overline{x}}^2$ would be replaced by $\nabla^2 = \partial_{\overline{x}}^2 + \partial_{\overline{y}}^2$. However, for the simplicity of the analysis and simulations in the present study, we confine ourselves to the problem posed on a one-dimensional field $0 < \overline{x} < \overline{L}$. We shall use a domain of length L, that is, $0 < \overline{x} < \overline{L}$ with

$$\frac{\partial}{\partial \overline{x}}\overline{n}_i = 0 \quad \text{at} \quad \overline{x} = 0, \overline{L} \quad \text{for} \quad i = 1, 2, 3. \tag{8}$$

Initially we assume that the Rhyncho are inserted at one end of the domain ($0 < \overline{x} < \overline{h} \ll \overline{L}$). Our initial conditions are thus

$$\overline{n}_i = \overline{n}_0 H(\overline{h} - \overline{x}) \quad \text{for} \quad i = 1, 2, 3. \tag{9}$$

We assume that the field $0 < \overline{x} < \overline{L}$ is divided up into M patches (possibly only one patch in the case of a monoculture planting), each of width $\overline{W} = \overline{L}/M$. This is illustrated in Figure 2.

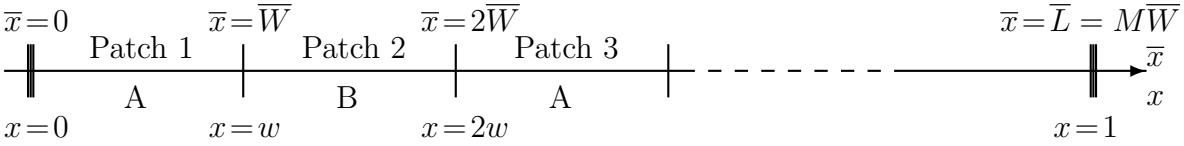

Figure 2: Illustration of 1-D field that we use for simulations together with notation for field and patch boundaries; dimensional notation is given above the horizontal line and nondimensional notation below the line.

2.4 Nondimensionalisation of model

Since the model has many parameters, it is useful to rescale all quantities so that variables have typical size of 1; this will also help identify if any processes are negligible or dominant. This process is called nondimensionalisation and here we assign

$$\overline{t} = \overline{T}t, \quad \overline{x} = \overline{L}x, \quad \overline{n}_j(\overline{x}, \overline{t}) = \overline{n}_{\max} n_j(x,t) \quad \text{for} \quad j = 1, 2, 3, \tag{10}$$

where L is the width of the field, we find that

$$\frac{\partial}{\partial t}n_j(x,t) = \frac{\overline{T}\,\overline{D}}{\overline{L}^2}\frac{\partial^2}{\partial x^2}n_j - \overline{\lambda}\,\overline{T}n_j + \overline{\alpha}_j^{A,B}\overline{T}n_j(1 - n_1 - n_2 - n_3). \tag{11}$$

We have chosen to nondimensionalise lengths by the width of the field in order that we can investigate what effect changing the size of the diffusion term has on the spread of the pathogen whatever the patch size. Alternatively, we could have non-dimensionalised lengths by the width of the patch, W.

The one dimensional equation for n_1 is

$$\frac{\partial}{\partial t}n_j(x,t) = D\frac{\partial^2}{\partial x^2}n_j - n_j + \alpha_j^{A,B}n_j(1-n_1-n_2-n_3), \tag{12}$$

where

$$D = \frac{T\overline{D}}{L^2}, \quad \overline{T} = \frac{1}{\overline{\lambda}}, \quad \alpha_j^{A,B} = \overline{\alpha}_j^{A,B}\overline{T}, \quad w = \frac{\overline{W}}{\overline{L}}, \quad h = \frac{\overline{h}}{\overline{L}}, \quad n_0 = \frac{\overline{n}_0}{\overline{n}_{\max}}, \tag{13}$$

while equations for n_2 and n_3 are similar. Equation (12) is subject to the initial conditions $n_j(0) = n_0H(h-x)$ and the boundary conditions $\partial_x n_j = 0$ at $x = 0, 1$; at the inter-patch boundaries $x = mw$, $m = 1, 2, 3\ldots$ illustrated in Figure 2 we have continuity of n_j, that is the conditions $n_j(w^-) = n_j(w^+)$ and $\partial_x n_j(w^-) = \partial_x n_j(w^+)$ hold.

2.5 Steady states of model

In general, the dynamics of partial differential equations such as (12) are complicated, and so a first stage in identifying their behaviour is to find any possible steady-states they may possess. After this, we determine the stability of such states to see if they may be attracting or repelling; later we will analyse how any stable steady-states may be approached.

Initially let us focus on just one species of crop, and so drop the A, B superscripts from α. At steady state we have

$$\begin{aligned} -n_1 + \alpha_1 n_1(1-n_1-n_2-n_3) &= 0, \\ -n_2 + \alpha_2 n_2(1-n_1-n_2-n_3) &= 0, \\ -n_3 + \alpha_3 n_3(1-n_1-n_2-n_3) &= 0. \end{aligned} \tag{14}$$

In general this system has two types of steady-state, the zero solution in which $n_1 = n_2 = n_3 = 0$ and three steady states in which one species of pathogen dominates to the complete exclusion of all others, that is, $n_j = 1 - 1/\alpha_j$ whilst the other two n_j variables are zero. In order to be physically relevant, these non-zero steady-states require the corresponding α_j to satisfy $\alpha_j > 1$. These general steady-states are summarised in the top four rows of Table 3.

Note that in the very special case $\alpha_1 = \alpha_2 = \alpha_3$, there is an additional two-parameter family of steady-state solutions given by

$$n_1^* = \theta_1\left(1-\frac{1}{\alpha}\right), \quad n_2^* = \theta_2\left(1-\frac{1}{\alpha}\right), \quad n_3^* = (1-\theta_1-\theta_2)\left(1-\frac{1}{\alpha}\right), \tag{15}$$

where $\theta_1, \theta_2 > 0$, $\theta_1+\theta_2 < 1$. Furthermore in the special cases that two of the α_j's are equal, there is a one-parameter family of steady-states in which the corresponding n_j's are of the form $\theta(1-1/\alpha)$ and $(1-\theta)(1-1/\alpha)$ for $0 < \theta < 1$ and the remaining $n_j = 0$. These cases are summarised in the last four lines of table 3; as before, these states are only physically relevant if the corresponding $\alpha > 1$.

Type	n_1	n_3	n_3	Conditions
zero	0	0	0	-
pure-1	1 - $1/\alpha_1$	0	0	-
pure-2	0	1 - $1/\alpha_2$	0	-
pure-3	0	0	1 - $1/\alpha_3$	-
coexistence-2-3	0	$\theta(1-1/\alpha_2)$	$(1-\theta)(1-1/\alpha_2)$	$\alpha_2=\alpha_3$, $0<\theta<1$
coexistence-1-3	$\theta(1-1/\alpha_1)$	0	$(1-\theta)(1-1/\alpha_1)$	$\alpha_1=\alpha_3$, $0<\theta<1$
coexistence-1-2	$\theta(1-1/\alpha_1)$	$(1-\theta)(1-1/\alpha_1)$	0	$\alpha_1=\alpha_2$, $0<\theta<1$
coexistence-1-2-3	$\theta_1(1-1/\alpha_1)$	$\theta_2(1-1/\alpha_1)$	$(1-\theta_1-\theta_2)(1-1/\alpha_1)$	$\alpha_1=\alpha_2=\alpha_3$, $\theta_1>0$, $\theta_2>0$, $\theta_1+\theta_2<1$.

Table 3: Classification of steady-state solutions

2.6 Stability of the steady states

In order to determine whether the steady-states will be observed in practise, we need to determine their stability. We do this by linearising about them, finding the Jacobian

$$\mathbf{J} = \begin{pmatrix} -1+\alpha_1(1-2n_1-n_2-n_3) & -\alpha_1 n_1 & -\alpha_1 n_1 \\ -\alpha_2 n_2 & -1+\alpha_2(1-n_1-2n_2-n_3) & -\alpha_2 n_2 \\ -\alpha_3 n_3 & -\alpha_3 n_3 & -1+\alpha_3(1-n_1-n_2-2n_3) \end{pmatrix}. \quad (16)$$

Eigenvalues of this matrix determine the stability properties of the steady-state.

The trivial steady-state at (0,0,0)

Here, the Jacobian is given by

$$\mathbf{J}_0 = \begin{pmatrix} \alpha_1-1 & 0 & 0 \\ 0 & \alpha_2-1 & 0 \\ 0 & 0 & \alpha_3-1 \end{pmatrix},$$

which has the eignevalues α_1-1, α_2-1, α_3-1, so is stable if $\alpha_1, \alpha_2, \alpha_3 < 1$, and unstable otherwise.

The pure n_1 steady-state at $(1-1/\alpha_1, 0, 0)$

Here the Jacobian is given by

$$\mathbf{J}_1 = \begin{pmatrix} 1-\alpha_1 & 1-\alpha_1 & 1-\alpha_1 \\ 0 & \frac{\alpha_2}{\alpha_1}-1 & 0 \\ 0 & 0 & \frac{\alpha_3}{\alpha_1}-1 \end{pmatrix},$$

which has the eignevalues $1-\alpha_1$, α_2/α_1-1, α_3/α_1-1, so is only stable if $\alpha_1 > 1$ and $\alpha_2, \alpha_3 < \alpha_1$.

The pure n_2 steady-state at $(0, 1-1/\alpha_2, 0)$

Here the Jacobian is given by

$$\mathbf{J}_2 = \begin{pmatrix} \frac{\alpha_1}{\alpha_2}-1 & 0 & 0 \\ 1-\alpha_2 & 1-\alpha_2 & 1-\alpha_2 \\ 0 & 0 & \frac{\alpha_3}{\alpha_2}-1 \end{pmatrix},$$

which has the eignevalues $1-\alpha_2$, α_1/α_2-1, α_3/α_2-1, so is only stable if $\alpha_2 > 1$ and $\alpha_1, \alpha_3 < \alpha_2$.

The pure n_3 steady-state at $(0, 0, 1 - 1/\alpha_3)$

Here the Jacobian is given by

$$\mathbf{J}_3 = \begin{pmatrix} \frac{\alpha_1}{\alpha_3} - 1 & 0 & 0 \\ 0 & \frac{\alpha_2}{\alpha_3} - 1 & 0 \\ 1 - \alpha_3 & 1 - \alpha_3 & 1 - \alpha_3 \end{pmatrix},$$

which has the eignevalues $1 - \alpha_3$, $\alpha_2/\alpha_3 - 1$, $\alpha_1/\alpha_3 - 1$, so is only stable if $\alpha_3 > 1$ and $\alpha_1, \alpha_2 < \alpha_3$.

Summary

If $\alpha_1, \alpha_2, \alpha_3 < 1$ then only the zero state is stable and all the others are not physically realisable; this corresponds to the crop being resistant to all species of pathogen, and is not expected; or such diseases are not of concern. We are only interested in minimising the effect when diseases are able to take hold of a crop.

If $\alpha_1 > 1 > \alpha_2, \alpha_3$ then only the pure n_1 steady-state is stable and the other two are not physically realisable, and the zero solution is unstable. Similarly if $\alpha_2 > 1 > \alpha_1, \alpha_3$ then only the pure n_2 state is stable, and if $\alpha_3 > 1 > \alpha_1, \alpha_2$ then only the pure n_3 state is stable. These correspond to one of the pathogen species being dominant.

If $\alpha_1, \alpha_2 > 1 > \alpha_3$ then the pure n_3 solution is not realisable, the zero solution is unstable, and only one of the pure n_1 and pure n_2 solutions can be stable even though both are physically relevant. The stable one corresponds to whichever has the larger α_j parameter. Thus again we have only one stable steady-state, similar results hold for the cases $\alpha_1, \alpha_3 > 1 > \alpha_2$ and $\alpha_2, \alpha_3 > 1 > \alpha_2$.

For $\alpha_1, \alpha_2, \alpha_3 > 1$ all three pure states are relevant, but only one is stable, and that is the one that corresponds to the largest value of α_j.

The above describes the generic situation. Below we address some degenerate cases which may occur if some of the growth rates α_j happen to be identical; these are special cases, and we start with the most rare case where all three rates are the same, before progressing to the less degenerate case where only two are identical and the third distinct.

The triple coexistence states at $(\theta_1(1 - 1/\alpha), \theta_2(1 - 1/\alpha), (1 - \theta_1 - \theta_2)(1 - 1/\alpha))$

Since these states only exist if $\alpha_1 = \alpha_2 = \alpha_3$, we drop the subscript. Here the Jacobian is given by

$$\mathbf{J}_{123} = \begin{pmatrix} \theta_1(1-\alpha) & \theta_1(1-\alpha) & \theta_1(1-\alpha) \\ \theta_2(1-\alpha) & \theta_2(1-\alpha) & \theta_2(1-\alpha) \\ (1-\theta_1-\theta_2)(1-\alpha) & (1-\theta_1-\theta_2)(1-\alpha) & (1-\theta_1-\theta_2)(1-\alpha) \end{pmatrix}, \tag{17}$$

whose eigenvalues satisfy

$$\lambda^3 - (1-\alpha)\lambda^2 = 0, \tag{18}$$

hence $\lambda = 0, 0, 1 - \alpha$. These states are thus marginally stable if $\alpha > 1$ and unstable if $\alpha < 1$. Their stability is 'marginal' since the zero eigenvalue indicates that some perturbations will not lead to a temporal growth, merely to the adjustment to another steady state from the family of steady states. Since this family is two dimensional there are two zero eigenvalues.

The double coexistence states at $(\theta(1-1/\alpha_1),(1-\theta)(1-1/\alpha_1),0)$

This case requires $\alpha_1 = \alpha_2 > 1$, the inequality being necessary for the population sizes to be positive. Here the Jacobian is given by

$$\mathbf{J}_{123} = \begin{pmatrix} \theta(1-\alpha_1) & \theta(1-\alpha_1) & \theta(1-\alpha_1) \\ (1-\theta)(1-\alpha_1) & (1-\theta)(1-\alpha_1) & (1-\theta)(1-\alpha_1) \\ 0 & 0 & \frac{\alpha_3}{\alpha_1}-1 \end{pmatrix}, \tag{19}$$

whose eigenvalues are $\lambda = 0, 1-\alpha_1, \alpha_3/\alpha_1 - 1$. This state is marginally stable if $\alpha_1 > 1$ and $\alpha_3 < \alpha_1$. If $\alpha_1 < 1$ then the states are no longer physically realisable, and if $\alpha_3 > \alpha_1$ then the pure n_3 state becomes stable and this loses stability. Similar results hold for the double coexistence states when $\alpha_3 = \alpha_2$ or $\alpha_3 = \alpha_1$. In all cases, for any given set of parameter values, we only ever find one state (or family of steady-states) is stable.

2.7 Fisher-KPP theory

A simple model of logistic growth of a population is given by

$$\frac{\mathrm{d}u}{\mathrm{d}t} = au\left(1 - \frac{u}{u_{\max}}\right), \tag{20}$$

where small populations grow exponentially ($\dot{u} \sim au$), but there is a maximum population size $u = u_{\max}$ above which growth is not possible.

Extending this model to a spatial domain (from $u(t)$ to $u(x,t)$) we obtain

$$\frac{\partial u}{\partial t} = D\frac{\partial^2 u}{\partial x^2} + au - bu^2. \tag{21}$$

This is the well-known Fisher-KPP model [1, 2], which has steady-state solutions of the form $u = 0$ and $u = a/b$, that is, constant in x. Assuming $a > 0$ then $u = 0$ is an unstable steady-state and $u = a/b$ is stable. There are travelling waves which join these states, that is $u = u(x-ct) = u(z)$ with $u \to a/b$ as $z \to -\infty$ and $u \to 0$ as $z \to +\infty$. Solutions of this form cannot be expressed explicitly in terms of elementary functions; however, phase plane analysis shows that the speed will always exceed $c_0 = 2\sqrt{aD}$. The form of the wave is illustrated in the left-hand panel of Figure 3.

The minimum speed c_0 can also be found using WKBJ methods as follows: we analyse the leading edge of the wavefront using

$$u(x,t) \sim \mathrm{e}^{w(x,t)}\left(A(x,t) + A_1(x,t) + \ldots\right), \tag{22}$$

where w is assumed to be the leading order term, and A a first correction, etc. Using x, t subscripts to denote partial derivatives, we find

$$\frac{A_t}{A} + w_t = a - bAe^w + D\frac{A_{xx}}{A} + D\frac{2A_x w_x}{A} + Dw_x^2 + Dw_{xx}, \tag{23}$$

from which the leading order terms (in $x/t \gg 1$) are

$$w_t = Dw_x^2 + a. \tag{24}$$

This equation has the similarity solution $w(x,t) = tF(\eta)$ where $\eta = x/t$, giving the first order ordinary differential equation $F - \eta F' = a + D(F')^2$. This is Clairaut's equation, which has both

general solutions and a singular solution. Both can be found by differentiating to obtain a second order ODE

$$0 = (\eta + 2DF')F''. \tag{25}$$

The general solutions have the form $F = p\eta + a + Dp^2$ for arbitrary constant p; whilst the singular solution is $F = a - \eta^2/4D$ and has no arbitrary constant. These correspond to general solutions for w of the form $w = px + t(a + p^2 D)$, which are travelling waves with speed $c = pD + a/p$, which has a minimum of

$$c_0 = 2\sqrt{aD}, \tag{26}$$

at $p = p_{min} = \sqrt{a/D}$. The singular solution has the form $w = (4Dat^2 - x^2)/4Dt$ which has the speed c_0. This is the expected solution, since it has more rapidly decaying shape than the general solutions; to obtain one of the other solutions, the initial conditions need to be carefully chosen so as to ensure the correct form of decay at the leading edge of the waveform.

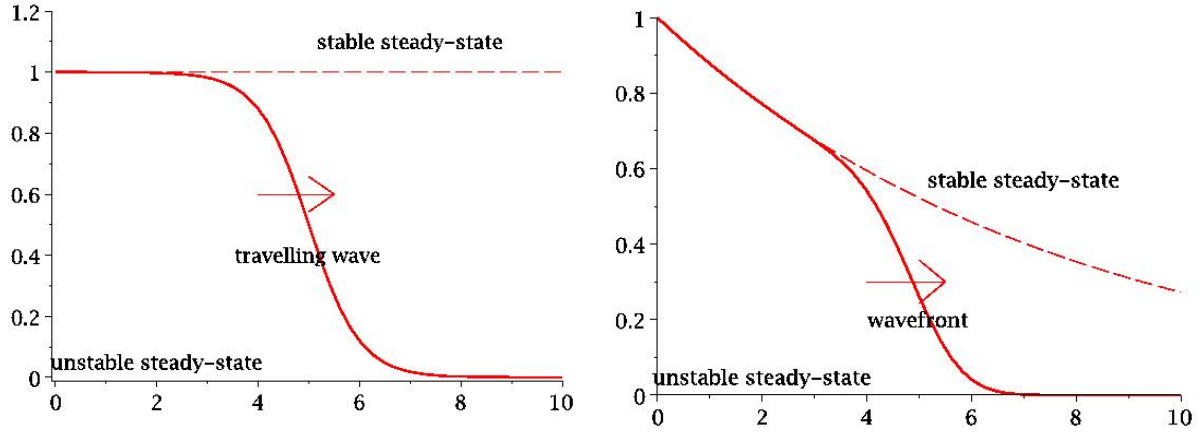

Figure 3: Illustration of approach to steady-state solutions in the Fisher-KPP equation. On the left, a travelling wave leads to the establishment of the stable steady-state solution from the unstable steady-state; on the right a modified travelling wave causes the concentrations to rise from the unstable zero solution to the stable steady-state which is exponentially in x.

The above has implicitly assumed that $a > 0$, which corresponds to a region where the population grows to a stable steady-state. We now turn to the case where the population dies out, that is, a region in which $a < 0$. Since we will later want to consider both regimes simultaneously, let us now use $\widetilde{a}$.

In the case $\widetilde{a} < 0$, the steady-state solution of (21) decays with increasing x. For example, in the case $b = 0$, it can be given explicitly as $u = u_0 \exp(-x\sqrt{-\widetilde{a}/D})$. The form of such a solution is illustrated in the right-hand panel of Figure 3. For $b \neq 0$, we note that the solution has the form

$$\widetilde{u} = \frac{-3\widetilde{a}}{2b}\mathrm{csch}^2\left(\frac{(x-x_0)}{2}\sqrt{\frac{-\widetilde{a}}{D}}\right) \sim C\exp\left(-x\sqrt{\frac{-\widetilde{a}}{D}}\right); \tag{27}$$

the latter approximation being for larger $(x - x_0)\sqrt{-\widetilde{a}/D}$, the arbitrary constant C replacing x_0. In order to determine the stability of this solution and the zero solution, we transform to $u(x,t) = \widetilde{u}(x)v(x,t)$ to obtain

$$\frac{\partial v}{\partial t} = D\frac{\partial^2 v}{\partial x^2} + b\widetilde{u}v - b\widetilde{u}v^2 - 2\frac{\partial v}{\partial x}\sqrt{-\widetilde{a}D}\coth\left(\frac{(z-z_0)}{2}\sqrt{\frac{-\widetilde{a}}{D}}\right). \tag{28}$$

If we consider the stability of the trivial solution $v = 0$ we find $v_t = b\widetilde{u}v$ hence $v = 0$ is unstable. The stability of steady-state $v = 1$ is determined by $w_t = Dw_{xx} - b\widetilde{u}w + 2Dw_x\widetilde{u}_x/\widetilde{u}$ which implies that $v = 1$ is stable. Assuming the region where $\widetilde{a} < 0$ is reasonably wide, $\widetilde{u} \to 0$ as $x \to w$, implies that the above equation (28) for v can be simplified to

$$\frac{\partial v}{\partial t} = -2\sqrt{-\widetilde{a}D}\frac{\partial v}{\partial x}, \tag{29}$$

hence the wavespeed can be seen to be $2\sqrt{-\widetilde{a}D}$ (note that $\widetilde{a} < 0$). In Figure 3 we also illustrate the manner in which this solution is approached.

In the application below we have consecutive patches where $a > 0$ and the solution $u = a/b$ constant is approached, followed by regions where $\widetilde{a} < 0$ and the decaying (csch^2) solution is approached. When this wave then meets the next area in which $a > 0$, there is a delay whilst the wave has to grow back from the decayed value towards a/b again. We now determine this timelag.

Let us ignore the diffusion term, and simply solve $u_t = au - bu^2$ subject to $u(0) = u_0$. This gives

$$u = \frac{au_0\mathrm{e}^{at}}{a + bu_0(\mathrm{e}^{at} - 1)}. \tag{30}$$

Now the time taken to grow from $u = u_0$ to u_1 is

$$t = \frac{1}{a}\log\left(\frac{u_1(a - bu_0)}{u_0(a - bu_1)}\right) = \frac{1}{a}\log\left(\frac{a}{bu_0} - 1\right). \tag{31}$$

Taking $u_1 = a/2b$, since the level only needs to grow to one half of its steady-state level for the wave to start moving, we obtain the latter simplification. For simplicity, we approximate $\widetilde{u}$ by an exponential, hence over the region of width w it drops from a/b to

$$u_0 = \frac{\widetilde{a}}{b}\exp\left(-w\sqrt{\frac{-\widetilde{a}}{D}}\right). \tag{32}$$

Hence we find the timelag

$$t_{\mathrm{lag}} = \frac{1}{a}\log\left(\mathrm{e}^{w\sqrt{-\widetilde{a}/D}} - 1\right) \approx \frac{w}{a}\sqrt{\frac{-\widetilde{a}}{D}}, \tag{33}$$

the latter approximation being for $w\sqrt{-\widetilde{a}/D} \gg 1$.

Combining the timelag with the time taken to travel, we find a combined time to travel across the two regions, each of width w is

$$T_{2w} = \frac{w}{2\sqrt{aD}} + \frac{w}{2\sqrt{-\widetilde{a}D}} + \frac{w}{a}\sqrt{\frac{-\widetilde{a}}{D}}, \tag{34}$$

from (26), (29) and (33), hence the average velocity is

$$c_{av} = \frac{4a\sqrt{-\widetilde{a}D}}{a - 2\widetilde{a} + \sqrt{-\widetilde{a}a}}. \tag{35}$$

2.8 Kinetics of the more general model

We now analyse the more general case of multiple populations

$$\frac{\partial n_1}{\partial t} = D\frac{\partial^2 n_1}{\partial x^2} - n_1 + \alpha_1 n_1(1 - n_1 - n_2), \tag{36}$$

$$\frac{\partial n_2}{\partial t} = D\frac{\partial^2 n_2}{\partial x^2} - n_2 + \alpha_2 n_2(1 - n_1 - n_2). \tag{37}$$

We use the same WKBJ asymptotic analysis, writing $n_1 = A_1 \exp w_1$, $n_2 = A_2 \exp w_2$ to obtain

$$w_{1,t} = \alpha_1 - 1 + D w_{1,x}^2, \qquad w_{2,t} = \alpha_2 - 1 + D w_{2,x}^2. \tag{38}$$

Now, writing $w_i = tF_i(\eta)$ for $\eta = x/t$ and $i = 1, 2$ we find

$$F_i - \eta F_i' = \alpha_i - 1 + D(F_i')^2, \tag{39}$$

hence we find the minimum velocities $c_i = 2\sqrt{(\alpha_i - 1)D}$.

From this analysis it is clear that wave equations are only possible when $\alpha > 1$. When $\alpha < 1$ solutions are expected to decay across the domain.

By linearising (36) so that

$$\frac{\partial n_1}{\partial t} = D\frac{\partial^2 n_1}{\partial x^2} - n_1 + \alpha_1 n_1, \tag{40}$$

steady state solutions of the form $n = A\exp(-\lambda x)$ can be found where

$$D\lambda^2 + \alpha - 1 = 0 \tag{41}$$

so

$$n = A\exp\left(-x\sqrt{\frac{1-\alpha}{D}}\right). \tag{42}$$

Take $\alpha > 1$ for a patch with plant type A and $\alpha < 1$ for a patch with plant type B for a pathogen n_1. The solution of (36) in the decaying domain will determine whether or not it can be effectively be considered extinct.

2.9 Numerical Results

For the three species of pathogen $i = 1, 2, 3$ we have

$$\frac{\partial n_i}{\partial t} = D\frac{\partial^2 n_i}{\partial x^2} - n_i + \alpha_{i\beta} n_i(1 - n_1 - n_2 - n_3), \tag{43}$$

where the infectivities are given by

$$\alpha_{i\beta} = \begin{cases} \alpha_{iA} & \text{if } 0 \le x < 1/4, \\ \alpha_{iB} & \text{if } 1/4 \le x < 1/2, \\ \alpha_{iA} & \text{if } 1/2 \le x < 3/4, \\ \alpha_{iB} & \text{if } 3/4 \le x < 1. \end{cases} \tag{44}$$

and $D = 1$. The linear domain $0 < x < 1$ is divided into four patches of equal widths with a different group variety, A or B, planted on each. α quantifies how adapted a strain of fungus n_i is to a particular type of crop, A or B. The boundary conditions are $\partial_x n_i = 0$ at $x = 0, 1$ for $i = 1, 2, 3$, and continuity of n_i at $x = 1/4$, $1/2$, $3/4$ with initial conditions $n_i(x, 0) = C\delta(x)$ where $C = 0.1$. Numerical simulations were carried out to establish behaviour patterns.

The monoculture: only one domain present $\alpha_{iA} = \alpha_{iB}$

The case where no strain is preferentially adapted to A or B but the strains might not be equally virulent can be modelled by choosing an α such as (45) or (46)

$$\alpha_{i\beta} = \begin{bmatrix} 1.2 & 1.2 \\ 0.5 & 0.5 \\ 0.1 & 0.1 \end{bmatrix}, \tag{45}$$

$$\alpha_{i\beta} = \begin{bmatrix} 2.2 & 2.2 \\ 1.2 & 1.2 \\ 0.5 & 0.5 \end{bmatrix}. \tag{46}$$

For (45) only strain 1 has a steady state solution, while for (46) strains 1 and 2 have steady state solutions. However, only the strain with the largest α has a stable nontrivial steady state solution. The other strains quickly decay both in time and across the domain. These results show how, as a model of different population competing for the same resources, only the outcome where one strain thrives is possible. When all strains have $\alpha < 1$ then no strains thrive.

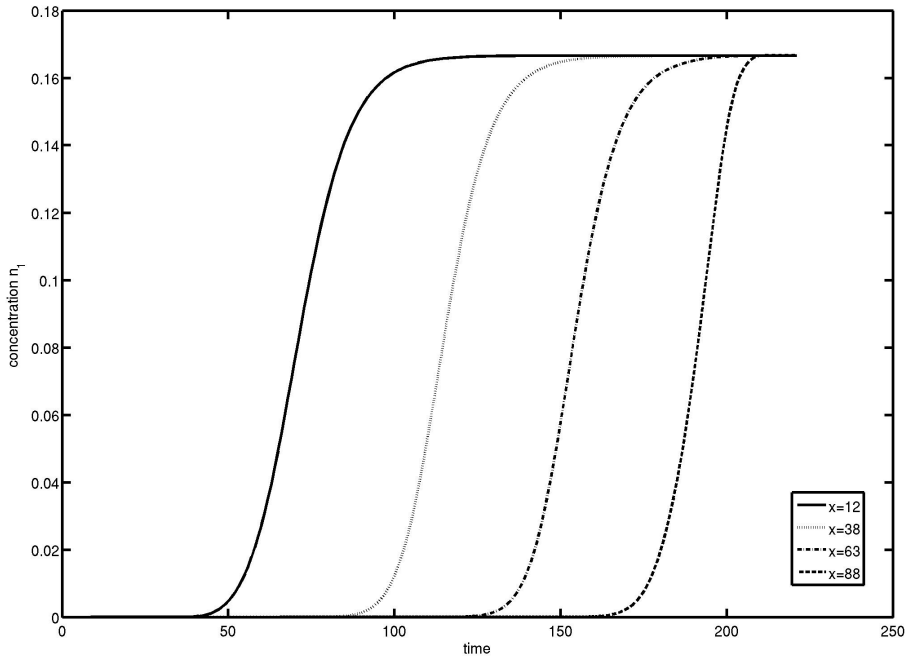

Figure 4: Solutions when α is as given in (45); progression of n_1 along x in time.

Figure 4 demonstrates how the travelling wave solution moves along the x direction with time. The speed of decay of the non-dominant strains depends on the value of α as is demonstrated in Fig.5.

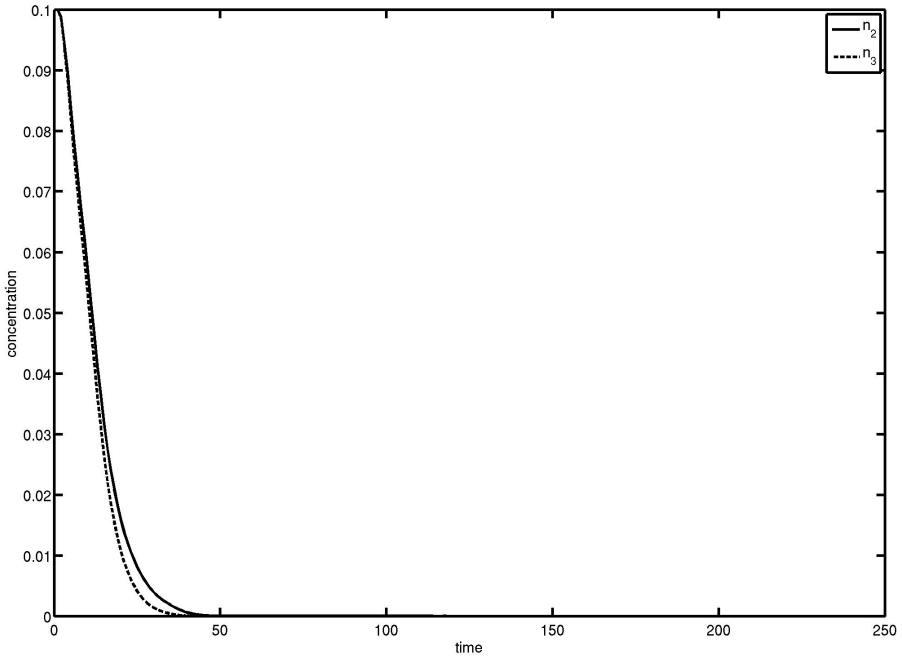

Figure 5: Solutions when α is as given in (45); decay of $n_2(1,t)$ and $n_3(1,t)$ with time.

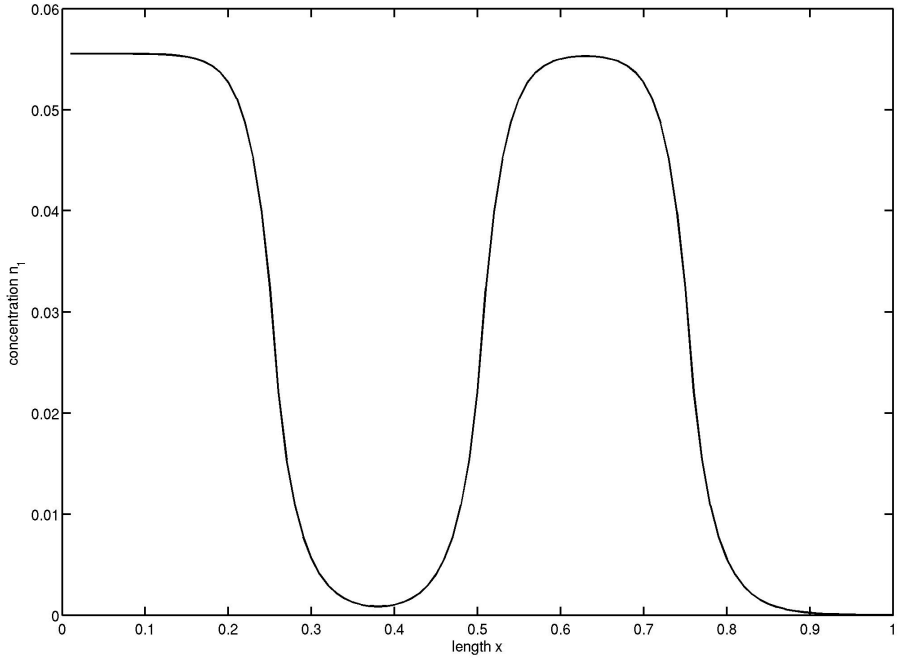

Figure 6: Steady state solutions when α is given by (47).

2.9.1 Patterned planting with only one strain present

If only one strain is present then α can be written as a vector. The steady state solutions when α is as given in (47) and (48) are plotted in Figures 6–7.

$$\alpha_\beta = \left[\begin{array}{cc} 1.2 & 0.9 \end{array} \right], \tag{47}$$

$$\alpha_\beta = \left[\begin{array}{cc} 2.2 & 1.2 \end{array} \right]. \tag{48}$$

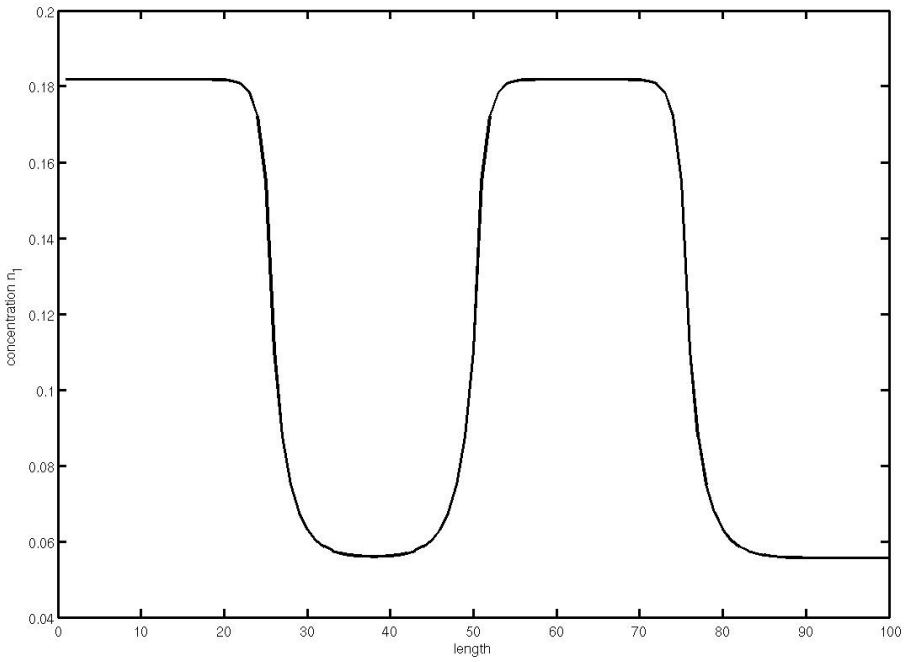

Figure 7: Steady state solutions when α is given by (48).

The steady state solution for α as given in (47) in Figure 6 has a maximum of 5.6×10^{-2} in the first quarter and 5.5×10^{-2} in the third. In the second and fourth quarters the concentration is $< 10^{-8}$. The steady state solution for α as given in (48) in Figure 7 has a maximum of 1.8×10^{-1} in the first and third quarters. Its minimum concentrations for the second and fourth quarters are 5.6×10^{-2}. The maximum concentration for a domain is approximately constant for a particular α, diffusion constant D and patch width W. The tops of the maxima at steady state are flat indicating the concentrations have reached their maximum possible values for these values of D and w.

For (47) the minimum t for which $n(0.75, t) > 0.01$ is ≈ 111. If the whole domain was only a homogenous patch of type A then this time would be ≈ 63. Dividing the domain into different patches slows down the rate of spreading.

2.9.2 Three strains and two domains

Two simple examples of α are (49) and (50). The corresponding steady state solutions can in found in Figures 8–9

$$\alpha_{i\beta} = \left[\begin{array}{cc} 1.2 & 0.01 \\ 0.01 & 1.2 \\ 0.1 & 0.1 \end{array} \right], \tag{49}$$

$$\alpha_{i\beta} = \begin{bmatrix} 2.2 & 0.01 \\ 0.01 & 1.2 \\ 0.1 & 0.1 \end{bmatrix}. \tag{50}$$

In Figure 8 the total concentration of n_1, n_2 and n_3 across the domain is almost constant while in Figure 9 it is not.

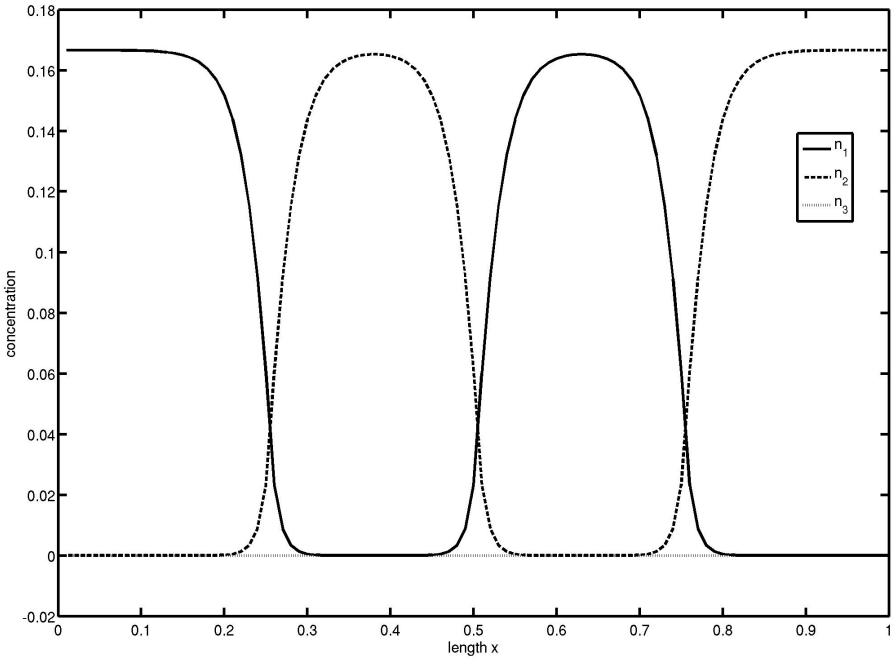

Figure 8: Steady state solutions when α is given by (49).

Now we take

$$\alpha_{i\beta} = \begin{bmatrix} 1.2 & 0.01 \\ 0.01 & 1.2 \\ 1.1 & 1.1 \end{bmatrix}. \tag{51}$$

The steady state solution is that of α given by (49). However, the transient solution is different.

A third strain can slow down the spreading of the virulent strain with a larger maximum value of α at the expense of an earlier initial infection time as the fungus spreads along the domain. Figure 12 is a surface plot of the full solution.

Figures 10–11 show examples of how a third strain can compete with two dominant ones. When α is given by (49) then $n_2(38,t) > 0.01$ when $t > 143$. When α is given by (51) then $n_2(38,t) > 0.01$ when $t > 206$. However, $n_3(38,t) > 0.01$ when $t > 80$. Similarly, when α is given by (49) then $n_1(63,t) > 0.01$ when $t > 172$. When α is given by (51) then $n_1(63,t) > 0.01$ when $t > 233$. However, $n_3(38,t) > 0.01$ when $t > 116$.

In Section 2.7 it was suggested that the decay of the concentration across the spatial domain at steady state is exponential. Figure 13 suggests that there is both exponential growth and decay when $\alpha < 1$ but not when $\alpha > 1$, as suggested in Figure 14.

A quick numerical experiment suggests that the solution (27) is accurate. Numerical results were obtained for $D = 0.25$, 0.5, 1, 2 and α is as given in (51). In the interval $0.25 \leq x < 0.5$ the

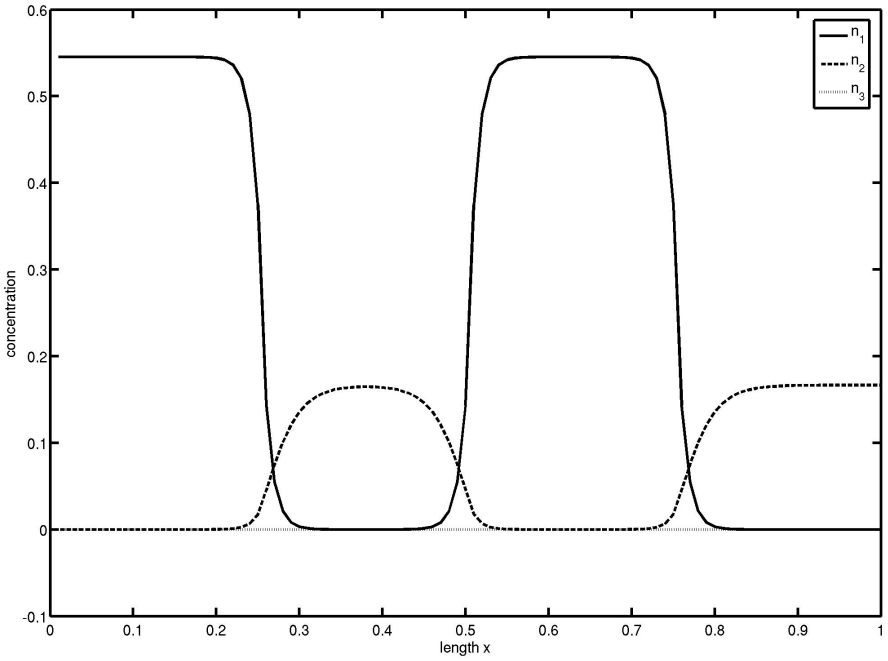

Figure 9: Steady state solutions when α is given by (50).

value of β was found when it was assumed that

$$\log(n_1) = A - \sqrt{\frac{\beta}{D}}. \tag{52}$$

It was found that $\overline{\beta} = 8.3 \times 10^3 \pm 5.6 \times 10^2$ which is approximately a constant suggesting that the decay is exponential.

Varying patch width

We take $\underline{\alpha}$ as in (47). Figure 15 shows how changing the patch width increases the frequency of the maxima and minima at steady state. It also shows how the shapes of the solutions change. At steady state there is both exponential growth and decay in the regions $\alpha < 1$ so that at the boundaries between the patches the value of the concentration is already close to its maximum. As the patches half in size, either the minimum concentration in the regions where $\alpha < 1$ decreases or the rate of change increases. If it is taken that $\log(n(x)) = -kx$ then the numerical results plotted in Fig.15 suggest that k approximately doubles as W is halved. As plant fields are much more coarse grained than a numerical model, there must be a maximum posible concentration gradient across a field and so a minimum value of W before the maximum and minima start to even out. There is a minimum W for which this type of planting pattern is more effective than mixing the two seed types up homogeneously before planting.

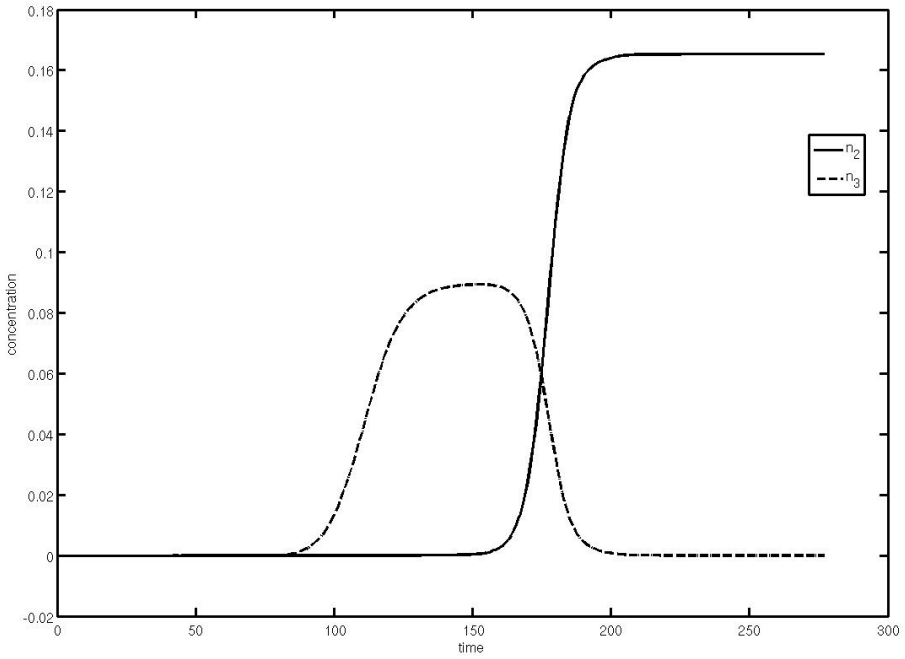

Figure 10: Steady state solutions when α is as given in (51): $n_2(38,t)$ and $n_3(38,t)$ against t.

3 Conclusions

A first attempt to identify the modelling requirements of this problem has been made. It has been recognised as a host-pathogen model which requires a spatial dimension to account for physical dispersal. The host-pathogen model has been decoupled and a pathogen-only model has been investigated. It has been assumed that the spread and growth of the fungus is not greatly affected by the damage it does to the plants.

After making some general observations on the coupled problem of crop growth in the presence of growing pathogen populations, we have focused on modelling the spread of pathogens. In particular we have concentrated our efforts on understanding why a patchwork planting of different species of a crop reduces the spread of pathogens. We have considered two species of crop and three species of pathogen and compared the spread of pathogen through a monoculture with that through a patchwork distribution of crop species. We find that because different species of crop have different resistances to the various species of pathogen, the spread through a mixed field is slower than through a monoculture. In a monoculture, once one species takes hold, it spreads without impediment; whilst in a patchwork pattern, at each boundary there is a time delay whilst a species which has been the less virulent in one patch grows to becomes more virulent in the next patch, and the species that was more virulent in one patch is less invasive in the adjacent patch.

As the patchsize is reduced we might expect this effect to be moderated, as seen in experiments; we have not yet carried out enough simulations or done enough analysis on the PDEs to understand the dependence on patch size. Investigating and optimising patch size would be the next goal in the future of this work.

The model quantifies the competitive advantage of one of three strains to one of two plant types. There is a critical value of α ($\alpha = 1$) for which any plant can thrive on any patch type.

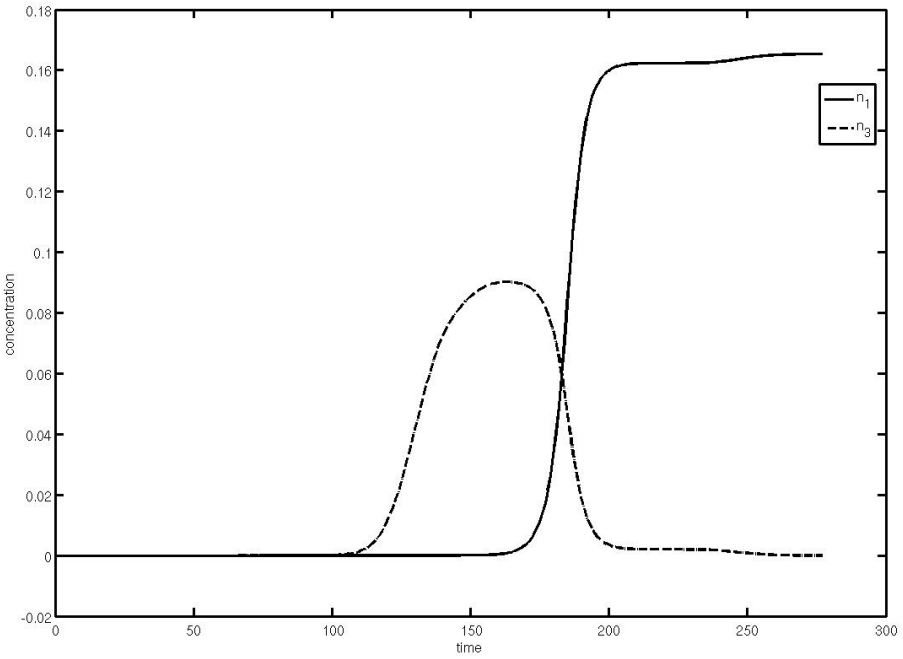

Figure 11: Steady state solutions when α is as given in (51): $n_1(63,t)$ and $n_3(63,t)$ against t.

Strains with less preferential adaptation to a plant type will spread across the whole domain faster than those with a more skewed adaptation and may slow co-existing strains with a more skewed adaptation down. It was found that at steady state the strains most preferentially adapted to a particular plant type will outcompete the other strains on that particular patch.

If the patch size is too small then the spores would not have adapted to that plant type by the time they move from one boundary to another. There will be no significant time delay when the spores spread across the boundary of two plant types. The time taken to adapt depends on the initial concentration of the spores with a competitive advantage on that plant type and the corresponding value of α. If W is too big the potential of slowing down the spread of the population has not been maximised. The time to move across can be calculated from the WKB analysis in Sections 2.7 and 2.8.

At steady state strains of a particular type are constrained to a particular patch. This pattern is reminiscent of the infection patterns of fungi after the initial spreading of the spores by the rain over winter. The temperature ensures that the population of fungus will not increase to a point where its growth is limited by the health or leaf area of the plants. However, this could be a factor to explain why the population distribution breaks out of this pattern during the rapid growth period in May/June. To model this period a more careful account must be made of the mass of healthy plant matter available to its fungal population, that is, the model should be parameterised for winter conditions and spring/summer conditions separately, or allow parameters to change with average temperature. The mass of healthy plant matter per unit area will depend on the area of healthy leaf per plant and the rate of dispersion will increase as plant height increases. If plants do not grow uniformily across the field the new conditions can be used to perturb the steady state solution of the initial model presented here.

The next step would be to accurately model α and understand how it relates to the physical

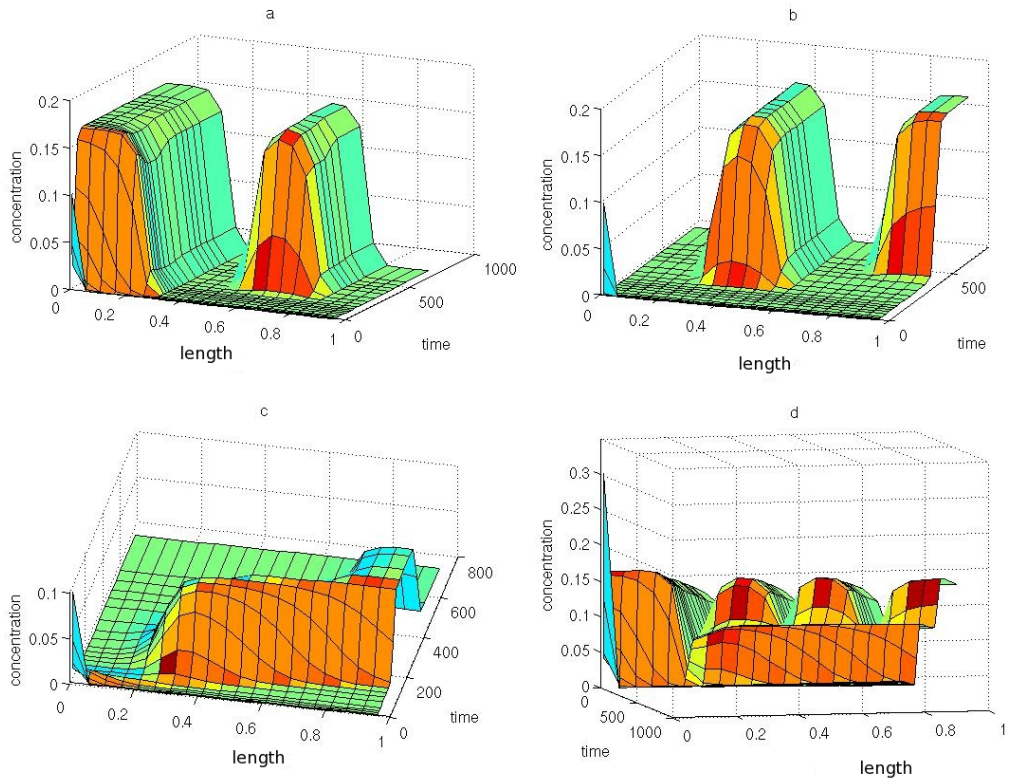

Figure 12: Surface plots of a) n_1 b) n_2 c) n_3 d) $n_{total} = n_1 + n_2 + n_3$

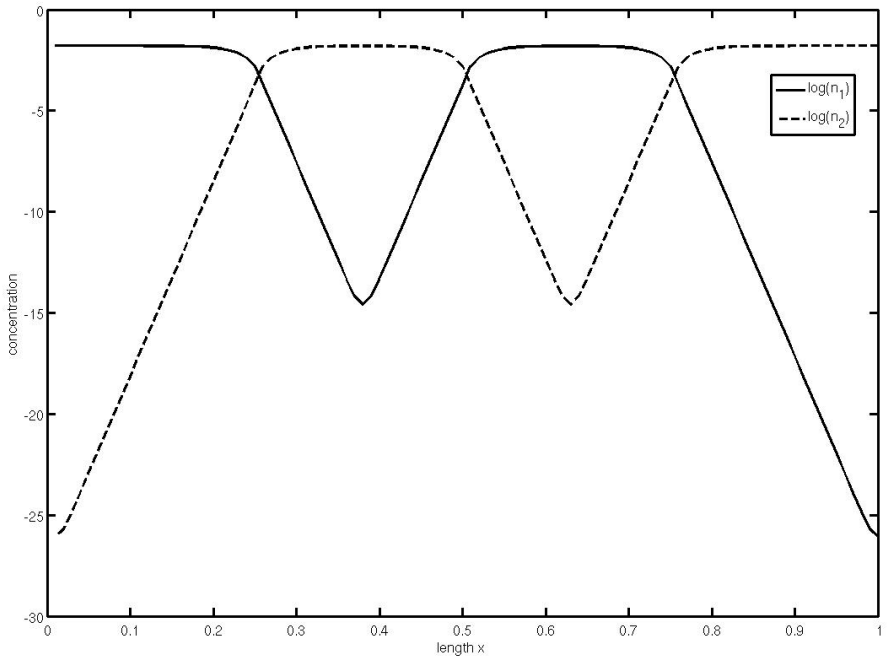

Figure 13: Log of steady state solutions when α is given by (47).

problem. The model suggests that there is a minimum value of α for which travelling wave solutions are possible so it would be helpful to know how to relate this threshold to observable behaviour.

References

[1] RA Fisher. The wave of advance of advantageous genes. *Ann Eugenics*, **7**, 355–369, (1937).

[2] AN Kolmogorov, IG Petrovskii & Piscounoff. A study of the equation of diffusion with increase in the quantity of matter, and its application to a biological problem. *Bjul. Mosk. Gos. Univ.*, **1**, 1–26, (1937). [English translation in P Pelce (ed.) 1988 Dynamics of Curved Fronts, Academic Press.]

[3] A Pielaat & F van den Bosch, A model for dispersal of plant pathogens by rainsplash. *IMA J Math Appl Med Biol*, **15**, 117–134, (1998).

[4] K Xi, T Turkington, J Meadus, J Helm & J Tewari. Dynamics of Rhynchosporium secalis pathotypes in relation to barley cultivar resistance. *Mycol Res*, **107**, 1485–1492, (2003).

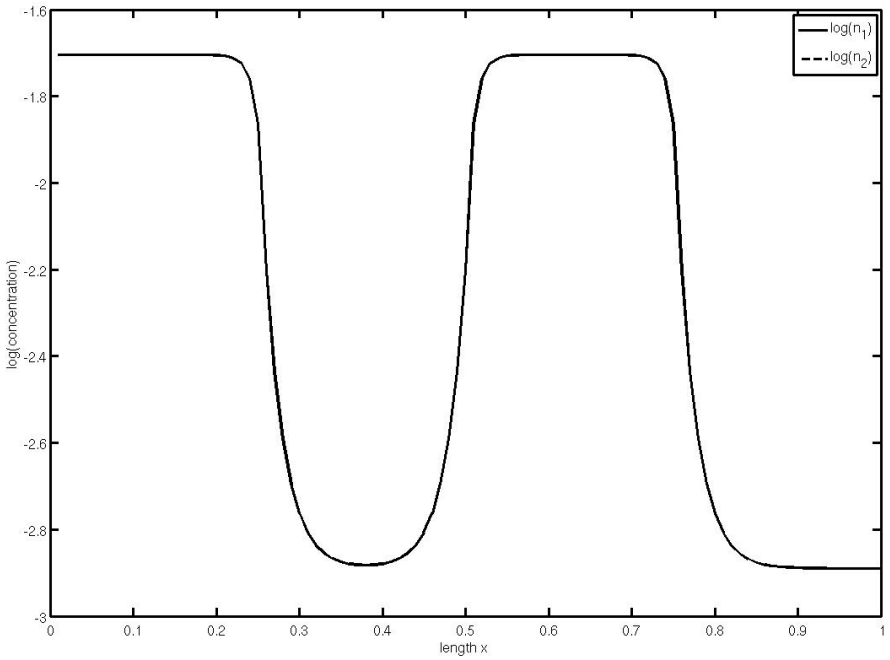

Figure 14: Log of steady state solutions when α is given by (48).

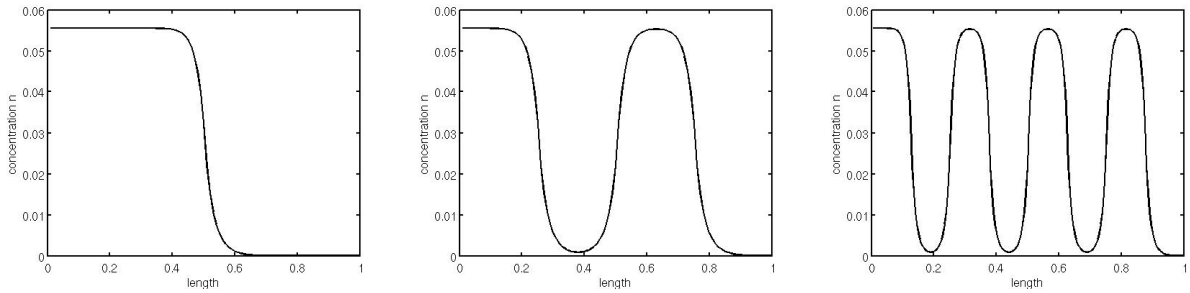

Figure 15: Steady state solutions for different patch widths W. From left to right: $w = 1/2, 1/4, 1/8$.